

# Strain rates in electrohydraulic forming of thin stainless-steel sheet metals

L. Langstädtler<sup>1,2,3\*</sup> and C. Schenck<sup>1,2,3</sup>

<sup>1</sup> University of Bremen, Bibliothekstraße 1, 28359 Bremen, Germany

<sup>2</sup> MAPEX – Center for Materials and Processes, 28354 Bremen, Germany

<sup>3</sup> bime – Bremen Institute for Mech. Eng., Badgasteiner Str. 1, 28359 Bremen, Germany

\*Corresponding author. Email: lasse.langstaedtler@uni-bremen.de

## Abstract

*Impulse forming technologies can be used for shaping thin sheet metal parts, e.g. bipolar plates for hydrogen production. Thereby, the energy transmission behaviour to the sheet metals depends on actual process characteristics. In electrohydraulic forming with exploding wire, shockwaves are expected to cause transient pressure fields onto the forming area. This transient force or pressure action realises the punch while the die is a rigid part of the tool. Hence, one part of the forming tool does not feature a defined geometry. To understand the impact of such kind of punches the resulting strain field was mapped during electrohydraulic forming experiments. Different explosion wire materials were used to form 100 µm thin EN 1.4404 / AISI 316L stainless-steel sheet metals. The displacement was measured in-process with two laser triangulation sensors at different positions. This time and space resolving data was taken to represent the initial pressure and resulting strain distribution. The in-process measurements enable further optimisation of the process settings.*

## Keywords

Electrohydraulic Forming, Energy Transmission, In-Process Measurement

## 1 Introduction

Electrohydraulic forming can be used for shaping thin sheet metal parts, e.g. for bipolar plates as used in hydrogen production. While the die is a rigid part of the tool like in conventional stamping, the punch is realised by a transient pressure field that is built up

instantaneously by an electrical underwater discharge. Various industrial applications have been demonstrated in recent years (Cantergiani et al., 2018; Golovashchenko et al., 2014). Electrical underwater discharge can be carried out with or without an explosion wire, although recent studies have observed an increase in pressure and repeatability when using an explosion wire (Eguia et al., 2011). In addition to the geometry, the properties of the wire material are also likely to determine the forming results and are therefore of interest for process optimisation. This was shown by experiments on the diameter of aluminium wires in electrohydraulic sheet metal forming (Langstädtler et al., 2018). A correlation was shown between the ratio of loading energy and calculated vaporisation energy and the forming result. Earlier investigations showed that the wire materials can have an influence on the explosion behaviour itself (Romanova et al., 2015). It was observed that the wire material changes the vaporisation process and the associated formation of shock waves in air (Rososhek et al., 2018). An increase in the forming result through the use of aluminium wires in electrohydraulic forming was attributed to the chemical potential of aluminium (Löffler et al., 2001). This raises the question of how the wire material influences the energy transfer and the final forming result.

A fast method for high velocity mapping via photon doppler velocimetry was introduced for foil vaporization forming (Lee et al., 2018). Here, the velocities were determined at a single bulging point for impact welding.

In this paper, physical electrohydraulic forming tests were performed with annealed EN 1.4404 / AISI 316L stainless-steel sheet metals with initial thickness of 100  $\mu\text{m}$  using different exploding wire materials at different energy levels. The forming was measured in-process at two separated bulging points with two laser-triangulation distance sensors to detect the distribution of the arising pressure field.

## 2 Materials and Methods

### 2.1 Forming set-up

Electrohydraulic forming was performed with a pulsed-power machine. The pulsed-power machine consisted of a capacitor bank with a capacitance of  $C = 100 \mu\text{F}$  which was loaded by a power supply to a loading voltage of  $U_0 = 1.3 \text{ kV}$ . This resulted in a loading energy of  $E_C = 85 \text{ J}$ . By short-circuiting the capacitor bank by a high current switch (ignitron NL8900, National Electronics, LaFox, IL, USA) over a thin wire, a peak current arose which vaporized the 20 mm long wire resulting in an explosion that was usable for electrohydraulic forming. Stainless-steel sheets (EN 1.4404 / AISI 316L) with dimensions of  $100 \times 100 \text{ mm}^2$  and a thickness  $s_0$  of 100  $\mu\text{m}$ , were bulged with a milled die made of EN 1.4301 / AISI 304. The die enabled two simultaneous bulging operations by rectangular cut-outs of  $8 \times 16 \text{ mm}^2$  with 3 mm edge radius (see **Fig. 1**). The workpiece and the die were in contact, as the gap was set to 0 mm. A round blank holder with a diameter of 70 mm was used.

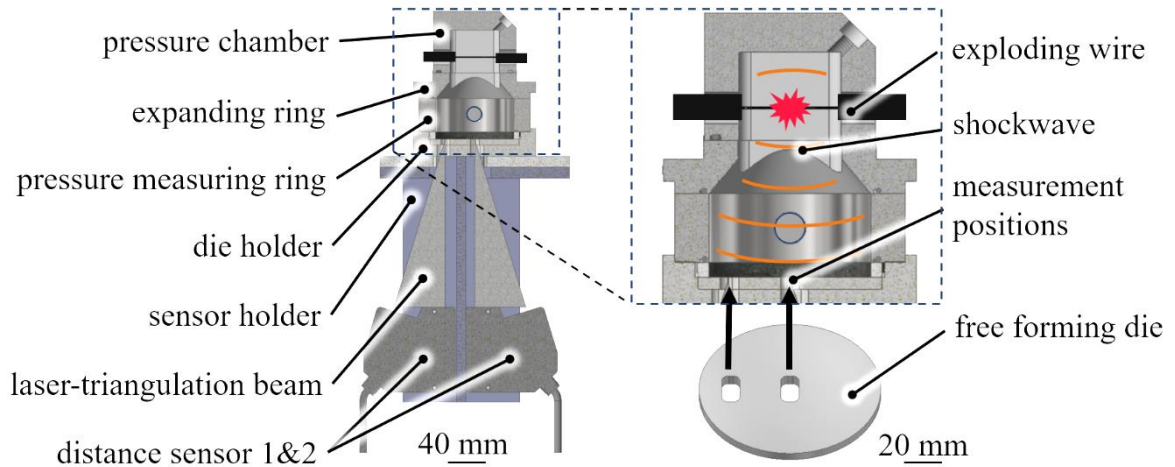


**Figure 1:** Forming set-up

## 2.2 Forming procedure

The material properties of the wires are given in **Table 1**. The loading energy  $E_C$  was set constant to 85 J. The quotient  $R$  of the loading energy and the vaporization energy  $E_V$  was kept constant to a value of  $R = 1.71 \pm 0.22$ . This was reached by adjusting the diameter for the different wire materials, see **Eq. 1** with  $\Delta h_v$  specific vaporization enthalpy,  $V$  volume of wire (depends on length and diameter) and  $\rho$  density of wire material. It is assumed that the wire can only evaporate completely when the necessary vaporization energy was provided. It should be noted here that the additional melting energy required was assumed to be negligible.

$$R = \frac{E_C}{E_V} = \frac{0.5 \cdot C \cdot U_0^2}{V \cdot \rho \cdot \Delta h_v} \quad (1)$$

Wire materials were pure aluminium (Al99.5), pure copper (Cu99) and pure tungsten (W99). The chosen wire diameter values were  $d(\text{Al99.5}) = 0.35$  mm,  $d(\text{Cu99}) = 0.28$  mm and  $d(\text{W99}) = 0.18$  mm. This resulted in vaporization energies  $E_V$  of  $E_V(\text{Al99.5}) = 57$  J,  $E_V(\text{Cu99}) = 52$  J and  $E_V(\text{W99}) = 44$  J and  $R$  values as  $R(\text{Al99.5}) = 1.49$ ,  $R(\text{Cu99}) = 1.63$  and  $R(\text{W99}) = 1.93$ , respectively. The tests for each wire material were repeated three times.

**Table 1:** Wire properties (matweb.com)

| wire property                               | unit | Al99.5 | Cu99 | W99  |
|---|------|--------|------|------|
| melting point $\theta$                      | °C   | 660    | 1083 | 3370 |
| boiling point                               | °C   | 2519   | 2562 | 5555 |
| specific vaporization enthalpy $\Delta h_v$ | kJ/g | 10.9   | 4.7  | 4.4  |

### 2.3 Measurement set-up

Two photoelectric sensors (LK-H157, Keyence, Osaka, Japan) were implemented for measuring the displacement  $h$  of the workpiece in the center (sensor 1) and 26 mm to the side (sensor 2) sampled every  $2.55 \mu\text{s}$  (see **Fig. 2**). This arrangement enabled a two-point insight into the arising pressure field. The measurement set-up was operated with a separate electrical potential (hv-disconnected) to reduce electrical interferences.

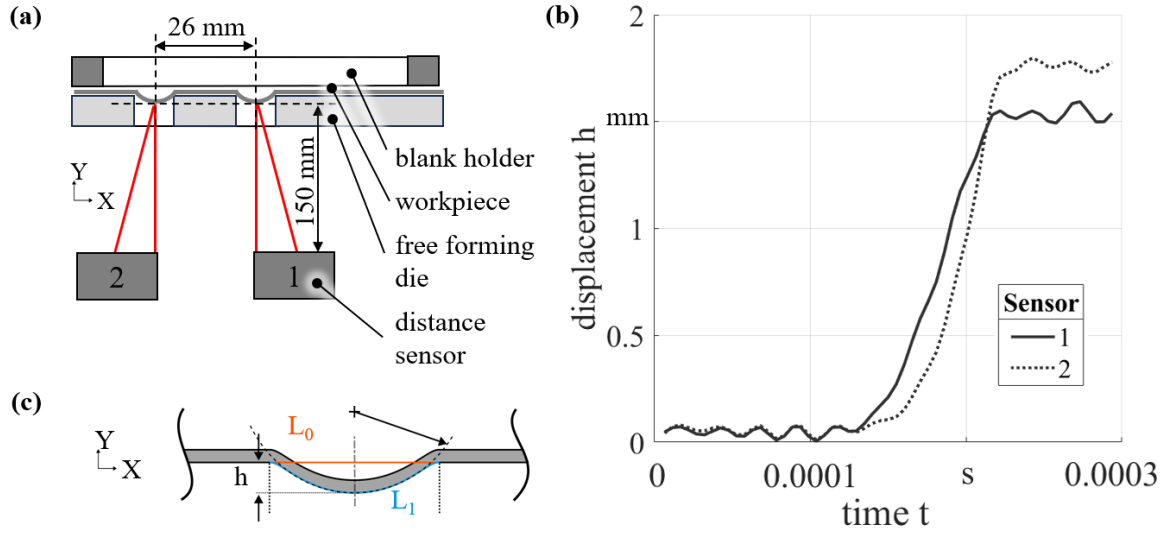


**Figure 2:** Measurement: (a) sketch of the set-up, (b) example (W99) measured displacement  $h$  versus time  $t$  and (c) definition of geometric measures for strain calculation

The signal of the displacement  $h$  versus time  $t$  was low-pass filtered with 50 kHz by minimum-order filter and a stopband attenuation of 60 dB. In connection with the shape in the X-Y-plane (cp. Fig. 2 (c)), the length of the surface segment  $L_1$  was calculated from the displacement  $h$ , **Eq. 2**. To calculate the strain  $\varepsilon_g$ , the length  $L_1$  was set in relation to the initial length  $L_0$  of  $L_0 = 8 \text{ mm}$  as given by the forming die (see **Eq. 3**). The strain rate  $\dot{\varepsilon}_g$  was determined by differentiate the strain  $\varepsilon_g$  over time  $t$ . The workpiece velocity  $v$  and its maximum were obtained by derivation of the displacement  $h$ . This method was introduced with a single sensor in the application of electromagnetic forming and laser shock forming (Langstädtler et al., 2024).

$$L_1 = \frac{\arctan\left(\frac{2 \cdot h}{L_0}\right) \cdot (4 \cdot h^2 + L_0^2)}{2 \cdot h} \quad (2)$$

$$\varepsilon_g = \frac{L_1 - L_0}{L_0} \quad (3)$$

### 3 Results

#### 3.1 Sheet metal displacement

The displacement varied for different wire materials while supplying the same amount of initial loading energy  $E_C$ , **Fig. 3**. The displacement curves were superimposed with an interference frequency resulting from the hv-disconnected power supply. The process time was in the range around 50-100  $\mu$ s. The lowest displacement was achieved with tungsten wires, Fig. 3a. Furthermore, differences in displacement in the center (sensor 1) and the side (sensor 2) were observed, whereas not only the maximum value, but also the curvature changed. The sheet metal starts to displace first in the center and then at the side with a delay of about 5-10  $\mu$ s.

Higher displacement  $h$  was measured for copper wires, Fig. 3b. A slight drag of the sensor 2 signal could also be detected here. It is assumed that the time difference in the displacement was caused by the presence of a non-uniform pressure propagation. This can be caused by differences in the explosion or by reflections on the chamber wall. However, the maximum displacement achieved was the same. Highest displacement was observed for aluminium wires, Fig. 3c. The increase of displacement at  $\approx 2.5$  mm with a change of curvature could be explained by a partial sheet metal fracture. Again, a slight drag and higher maximum value of the displacement at sensor 2 was detected.

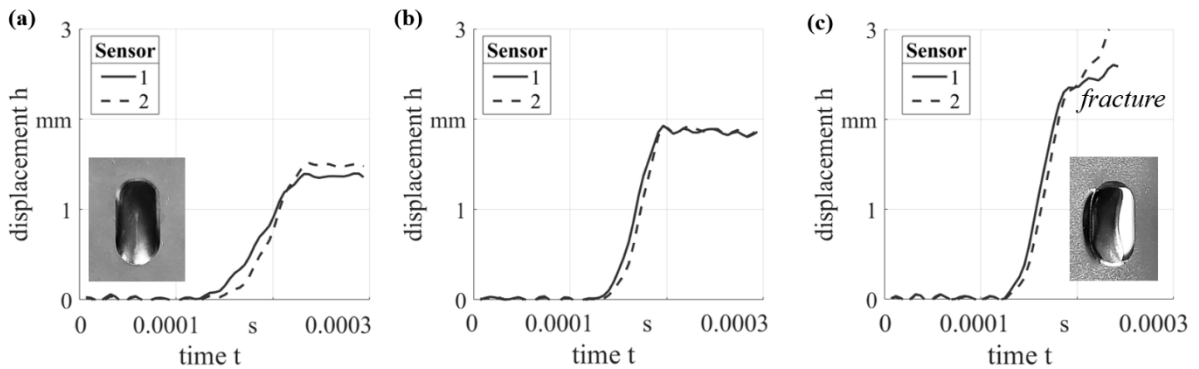


**Figure 3:** Example curve of displacement  $h$  versus time  $t$  for different wire materials ( $E_C = 85$  J): (a) W99, (b) Cu99 and (c) Al99.5

The maximum sheet velocity values  $v_{\max}$  were determined in the range of 30 m/s to 90 m/s depending on the exploding wire material. With tungsten wires (W99) the lowest values were observed, with higher values of around  $30 \pm 8$  m/s at sensor 2 compared to around  $25 \pm 8$  m/s at sensor 1. The fluctuations in the velocities occurred for tungsten wires were relatively high. Copper wires led to higher velocities up to  $55 \pm 4$  m/s. In addition, less difference in maximum velocity between the measurement in the center (sensor 1) and at the side (sensor 2) and less fluctuations could be detected. The highest sheet velocities were achieved with aluminium wires with up to 80 m/s (sensor 1:  $60 \pm 10$  m/s) with slightly higher velocity at the side (sensor 2;  $50 \pm 10$  m/s). Furthermore, the highest fluctuations occurred for aluminium wires. In addition to fluctuations in discharge, this is also attributed to the occasional fracture and cutting of the sheets due to higher pressure peaks.

### 3.2 Sheet metal strain and strain rate

As expected, the estimated strain and strain rates show similar behaviour as the discussed displacement and velocity. Maximum strains were determined at 0.05 to 0.15 for the different wire materials, **Fig. 4**. The detected failure of the stainless-steel sheets using aluminium wires was detected at 0.2 - 0.25 which correlates with expected fracture strains. Achieved strain rate values were in the range of 2000 and 8000 1/s, **Fig. 5**. Analogous to the sheet velocities, the lowest values were achieved for tungsten, increasing with copper and the highest strain rates using aluminium wires. In addition, the strain rates calculated with sensor 2 tend to be higher. An increase in strain rates is justified by the fact that the wire materials cause different pressure surges and different amounts of energy. As a result, aluminium wires have the highest pressure surge, which leads to higher energy transmission and higher strain rates.

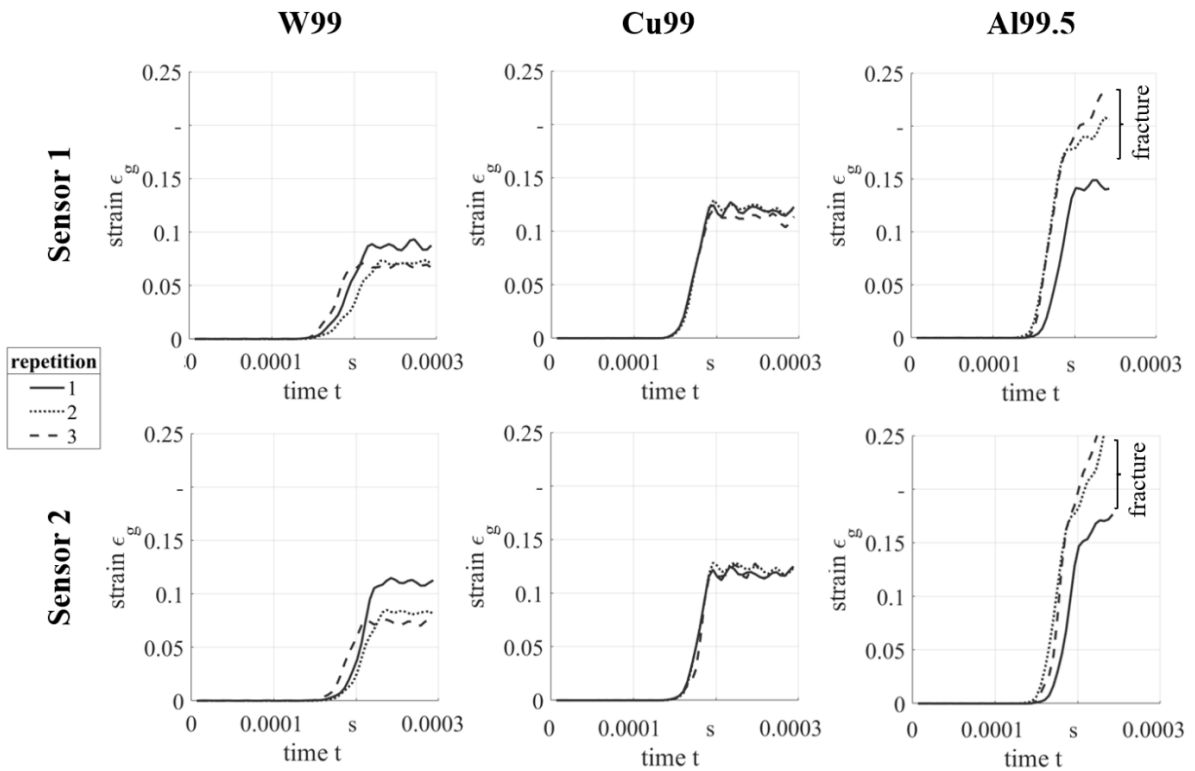


**Figure 4:** Strain  $\epsilon$  versus time  $t$  for different wire materials and positions ( $E_C = 85$  J)

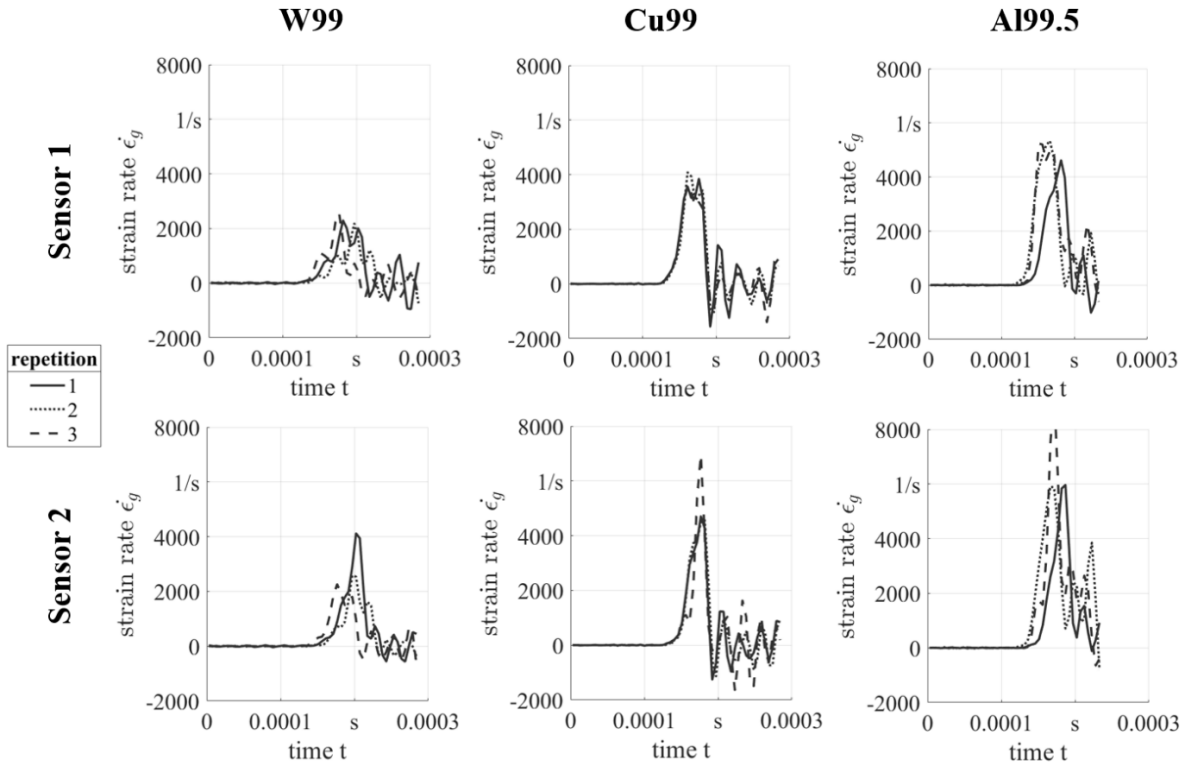


**Figure 5** Strain rate  $\dot{\epsilon}_g$  versus time  $t$  for different wire materials and positions ( $E_C = 85 \text{ J}$ )

## 4 Summary and conclusion

A in-process displacement measurement for investigation pressure fields of electrohydraulic forming was introduced in this paper. Interference effects on the measurement signal were reduced using a special power supply. The measuring system was equipped with two sensors to enable the measurement of two separate forming operations within the sheet plane. The tested wire materials had a significant influence on the process behavior of electrohydraulic forming thin stainless-steel sheet metals. The following conclusion could be drawn:

- Sheet metal velocities up to 80 m/s were measured
- Strain rates up to 8000 1/s were calculated
- Differences in displacement over time and maximum velocities as well as the strain and strain rates were observed depending on the wire material
- Gradients in the pressure field were detected which are related to the wire material

The gradients in the values may be caused through differences in the interacting pressure wave. Here, reflections and interferences in the pressure chamber could cause differences in the effect. It is also expected that the resulting gradients in the pressure fields could change depending on the R value which will be investigated in future work.

Aluminium wires showed the highest straining which could be related to the higher reactivity of the wire material. However, aluminium as well as tungsten wires tended to higher fluctuations and caused differences in the pressure fields. Therefore, it would be desirable to combine the positive properties of the wires such as reactivity with the stable behavior by using composite wires.

## Acknowledgments

The authors gratefully acknowledge the support by the German Research Foundation DFG for the project “Wirkmedienbasierte Impulsumformung von Kanalstrukturen”. This research was funded by the Deutsche Forschungsgemeinschaft (German Research Foundation - DFG), grant number 529030284.

## References

- E. Cantergiani E. et al., 2018. Example of two industrial Electro-hydraulic forming applications highlighting the advantages of high strain rates, Conference: NEBU NEHY.
- I. Eguia et al., 2011. Pressure Field Stabilisation in High-Voltage Underwater Pulsed Metal Forming Using Wire-Initiated Discharges, Key Engineering Materials Vol. 473.
- S. F. Golovashchenko et al., 2014. Pulsed electrohydraulic springback calibration of parts stamped from advanced high strength steel, Journal of Materials Processing Technology 214, 2796–2810.
- L. Langstädtler et al., 2018. Electrohydraulic incremental bulk metal forming, MATEC Web of Conferences, 190.
- L. Langstädtler et al., 2024. Strain rates in high velocity forming of foils, Materials Research Proceedings, Vol. 41, pp. 1527-1535.
- T. Lee et al., 2018. Proceedings of the International Conference on High Speed Forming, Columbus, OH.
- M. Löffler et al., 2001. Electrical wire explosion as a basis for alternative blasting techniques, Proceedings of the International Conference on Pulse Power Applications.
- V. M. Romanova et al., 2015. Electric Explosion of Fine Wires: Three Groups of Materials, Plasma Physics Reports, Vol. 41, No. 8, pp. 617-636.
- A. Rososhek et al., 2018. Phase transitions of copper, aluminum, and tungsten wires during underwater electrical explosions, Physics of Plasmas 25 (10).  
<https://matweb.com/>, data accessed at 04.04.2025. MatWeb online material property data base. MatWeb, LLC, 2020 Kraft Drive, Suite 3005, Blacksburg, VA 24060 USA.